Journal of Hazardous Materials 381 (2020) 120903

Contents lists available at ScienceDirect

Journal of Hazardous Materials

journal homepage: www.elsevier.com/locate/jhazmat

Indigenous strain *Bacillus* XZM assisted phytoremediation and detoxification of arsenic in *Vallisneria denseserrulata*

Sana Irshad[a], Zuoming Xie[a,b,*], Jia Wang[a], Asad Nawaz[c], Yan Luo[d], Yanxin Wang[a,b], Sajid Mehmood[e], Faheem[a]

[a] School of Environmental Studies, China University of Geosciences, Wuhan, 430074, PR China
[b] State Key Laboratory of Biogeology and Environmental Geology, China University of Geosciences, Wuhan, 430074, PR China
[c] College of Food Science and Technology, Huazhong Agricultural University, Wuhan, 430070, PR China
[d] Environmental Monitoring Station, Jianli Environmental Protection Bureau, Hubei Jianli 433300, PR China
[e] School of Civil Engineering Guangzhou University, Guangzhou, 510006, PR China

ARTICLE INFO

Editor: Rinklebe Jörg

Keywords:
Vallisneria denseserrulata
Subcellular distribution
Phytobial remediation
Arsenic metabolisation

ABSTRACT

The symbiosis between *Vallisneria denseserrulata* and indigenous *Bacillus* sp. XZM was investigated for arsenic removal for the first time. It was found that the native bacterium was able to reduce arsenic toxicity to the plant by producing higher amount of extra cellular polymeric substances (EPS), indole-3-acetic acid (IAA) and siderosphore. Interestingly, *V. denseserrulata-Bacillus* sp. XZM partnership showed significantly higher arsenic uptake and removal efficiency. The shift in FT-IR spectra indicated the involvement of amide, carboxyl, hydroxyl and thiol groups in detoxification of arsenic, and the existence of an arsenic metabolizing process in *V. denseserrulata* leaves. The scanning electron microscopy (SEM) images further confirmed that the bacterium colonized on plant roots and facilitated arsenic uptake by plant under inoculation condition. In plant, most of the arsenic existed as As(III) (85%) and was massively (> 77%) found in vacuole of particularly leaves cells. Thus, these findings are highly suggested for arsenic remediation in the constructed wetlands.

1. Introduction

Arsenic pollution has become worldwide environmental problem especially in arsenic contaminated freshwater ecosystems. Arsenic is required in trace amount for the proper functioning of digestive track in many rodents, birds, herbivore and many other animals including humans, but its excess exposure is poisonous (Soetan et al., 2010; Aljerf, 2018). More than 170 M people all over the world including China, Bangladesh, Chile, India, Pakistan, United States, Canada, Brazil, Indonesia, Mexico, Hungary and Vietnam are affected by arsenic toxicity. In Southeast Asia, about 100 M people are at the risk of arsenic poisoning (Duan and Zhu, 2018). A study estimated that 19.6 M people, in China alone, are at the risk of arsenic poisoning due to ground water contamination (Rodríguez-Lado et al., 2013).

In an uncontaminated environment, arsenic level is even less than 1 or 2 μg/l but its concentration can even increase up to 5000 μg/l, due to the weathering of arsenic containing sediments and volcanism, which is 500 times higher than arsenic drinking water guideline (10 μg/l) (W.H. Organization, 2011). Arsenic enters to human body via food or drinking water and causes chronic ailments such as liver and kidney disorders, skin lesions, brain cancer and digestive track poisoning (Deng and Guo, 2011). Leucomelanosis, melanosis, keratosis, dorsum, hyperkeratosis, oedema, non-petting skin cancer and gangrene are the most adverse ailments among the affected peoples. The inorganic arsenic is more toxic than organic arsenic, and among inorganic, As(III) is 60 time more toxic than As(V) (Chakraborty et al., 2014). However, organic arsenic is very rare and mostly present in shallow water. As(V) is main and thermodynamically stable chemical form of arsenic in toxic waters, while As(III) is found mainly in ground water (Bertolero et al., 1987).

Phytoremediation of arsenic contaminated water has emerged as one of the most promising and environment friendly technique against physical and chemical methods such as adsorption, precipitation, immobilizations, stabilization/solidification reverse osmosis etc. (Chen et al., 2017). It first came to light in 2001 when *Pteris vattita* was discovered by Ma et al. (2001) as arsenic hyper-accumulator. At present, many arsenic hyper-accumulators have been reported such as *Vallisneria neotropicalis* (Lafabrie et al., 2011) and *Holcus lanatus* (Hartley-Whitaker et al., 2001). Moreover, some macrophytes have also been testified to bio-accumulate arsenic (Chen et al., 2017). Although phytoremediation of arsenic is eco-friendly, still high arsenic

* Corresponding author at :School of Environmental Studies, China University of Geosciences, Wuhan, 430074, PR China.
E-mail address: zuoming.xie@cug.edu.cn (Z. Xie).

https://doi.org/10.1016/j.jhazmat.2019.120903
Received 14 June 2019; Accepted 15 July 2019
Available online 30 July 2019

concentration can inhibit plant growth.

As an assistant to numerous phytoremediation approaches and for making this technology more effectual, a number of scientific studies have been conducted for possible use of plant growth promoting (PGP) bacteria. These bacteria promote plant growth and catalyse the redox transformations (Xie et al., 2014) that are important for arsenic kinesis (Sun et al., 2018) and phytoremediation (Nie et al., 2002). PGP bacteria are well-known to confer a wide range of positive effects on plant growth and immunity, such as alteration of metal phytoavailability mechanisms in the rhizosphere, produce extracellular polymeric substances, indole-3-acetic acid, and siderosphore that increase plant growth and biomass, which in turn promote phytoremediation (Yang et al., 2012). After phytoextraction, subcellular distribution and chemical forms of arsenic are proposed to be connected with arsenic detoxification and tolerance in plants (Aljerf and AlMasri, 2018).

Still, research for finding new plant species with a worthy potential of arsenic remediation such as rapid growth rate, high biomass and arsenic accumulation and innate mechanism for arsenic detoxification is crucial for combating arsenic toxicity from environment (Prum et al., 2018). In short, there is a quest to find new arsenic hyper-accumulation plants (Meharg and Hartley-Whitaker, 2002) and PGP bacteria (Sun et al., 2018). Many of the *Vallisneria* species have already being used for the phytoremediation of arsenic contaminated water (Lafabrie et al., 2011; Iriel et al., 2015), but at the best of our knowledge *V. denseserrulata* has not yet been reported for arsenic bioremediation. Thus, the aim of this study was to explore the arsenic bioaccumulation and detoxification mechanism in indigenous aquatic plant *Vallisneria denseserrulata* (Makino). The exploration of PGP attributes of the indigenous strain *Bacillus* XZM and its symbiotic association with *V. denseserrulata* in a microcosm experiment for arsenic removal was also a part of this study. The study mainly focused on *Bacillus* XZM assisted uptake, metabolisation and bioaccumulation (subcellular level) of arsenic in *V. denseserrulata*.

2. Materials and methods

2.1. Bacterial isolation and identification

The indigenous strain *Bacillus* XZM was isolated from the aquifer of Shuangzhai village (Shanyin country, Dotong Basin located in Shanxi Province of China 39°21´N, 112°51´ S) as a part of our previously reported work (Xie et al., 2014). It has gene bank accession number of SUB4899103 BacillusMK271736. Strain was cultured in nutrient broth (NB) media (0.2% yeast extract, 0.5% peptone and 0.5% NaCl) at 32 °C overnight prior to further experimentation.

2.2. Determination of minimum inhibitory concentrations for Arsenite and Arsenate

The bacterial culture was streaked on solidified agar petri plates (NB + 2 g/l agar) containing arsenite [As(III)] (1–40 mM) and/or arsenate [As(V)] (10–150 mM). The plates were incubated at 32 °C for 5 days. The contamination or growth of other colonies was verified through reference plates that lack arsenic compounds.

2.3. Plant growth promoting (PGP) attributes of bacteria

The PGP attributes of bacterium XZM were determined in the presence of arsenic as an *in-vitro* experiment. Two levels of arsenic stress [0.25 ppm (L) and 2.5 ppm (H)] were prepared by adding sodium arsenate (Na_2HAsO_4) in respective growth media.

The indole acetic acid (IAA) synthesis by strain *Bacillus* XZM was determined as described by Gordon and Weber (1951). The EPS production was quantified according to Kazy et al. (2002). The culture was spread on petri plates with NB and agar. The number of colony forming units (CFU) was used as bacterial biomass. Siderosphore production was verified as Chromeazurol S (CAS; Sigma-Aldrich) oxidation according to Schwyn and Neilands (Schwyn and Neilands, 1987). (The detailed methods are provided as supplementary material as section 1S).

2.4. Determination of in vitro arsenate reduction potential

In order to determine the reduction potential of strain XZM, vials containing 5 mM As (V) in 50 ml of chemically modified media (KH_2PO_4 0.14 g/l, NaCl 1 g/l, KCl 0.5 g/l, $CaCl_2$ 0.13 g/l, $MgCl_2.6H_2O$ 0.62 g/l, NH_4Cl 0.25 g/l in 25 mM sodium acetate solution) were inoculated, and incubated at 32 °C for 72 h. At each sampling point OD and arsenic concentration were determined by spectrophotometer (UV-1800PC Spectrophotometer, MAPADA) and hybrid generation-atomic fluorescence spectroscopy (HG-AFS; AFS-830, Beijing Jitian Instrument Co., Ltd., Beijing, China), respectively (Le et al., 2000). Control vials without bacterial inoculation were used to address the abiotic arsenate reduction.

2.5. Experimental arrangements

2.5.1. Selection of Vallisneria denseserrulata

The aquatic plant *Vallisneria denseserrulata* (Makino) was obtained from Wuhan Botanical Garden, Chinese Academy of Sciences, Wuhan. The plant was grown in tap water for 10 days and tested for diverse heavy metal resistance [$HgCl_2$, $Cu(NO_3).23H_2O$, $NiCl_2.6H_2O$, Na_2HAsO_4, $Cd(NO_3).24H_2O$, $ZnCl_2$, Na_2SeO_4 and $Cr(NO_3)_3$] at a concentration of 2 ppm and growth inhibition was observed. The plant was able to tolerate As, Zn, Se and Hg while its growth was slightly inhibited under Cu, Ni, Cd, and Cr stress.

2.5.2. Microcosmic setup

The microcosms for arsenic experiment were established at 25 °C with 16 h photoperiod. For microcosms establishment, 8 litres of plant growth media (mixture of Na_2HAsO_4 in 1% Hogland solution) (Hoagland and Arnon, 1950) was added in each transparent tank. Four treatments were established as the following: 0.25 ppm As(V) (L), 2.5 ppm As(V) (H), 0.25 ppm As(V) + XZM (LB), and 2.5 ppm As(V) + XZM (HB). About 20 g of fresh plant biomass was planted in each treatment group with a bed of glass beads (2.5 mm diameter). The control microcosm (C) was without As(V) and bacterial inoculation. For inoculation purpose, the roots of *V. denseserrulata* were dipped in overnight grown bacterial culture (in NB media) for 3 min and further 10 ml of this culture was also added in each microcosm. In this way, an experiment of 10 microcosms with 5 treatments in duplicate was established. Approximately, 0.5 ml of liquid sample was collected every 36 h from each microcosm. The samples were filtrated (1 µm), preserved (0.5% HNO_3) and stored at − 20 °C in dark for further arsenic speciation.

The plants were harvested after 20 days. The harvested plants were washed with 0.01% EDTA and ultrapure water repeatedly and morphological properties were determined (details are provided as supplementary material as section 3S). Roots and shoots were separated and stored at -20 °C in dark for further analysis. Total nitrogen content in leaves was measured as previously defined by Horneck and Miller (1997) and total phosphorous was determined by colorimetric method (Fiske and Subbarow, 1925).

2.5.3. Chlorophyll determination

The fresh leaves were grinded with ice cooled ethanol and the absorbance of the resulting extract was measured at 663 and 645 nm (UV-1800PC Spectrophotometer, MAPADA) for quantification of chlorophyll *a* and *b*, respectively (Maclachlan and Zalik, 1963).

2.5.4. Oxidative stress determination

The root and shoot samples were used to monitor lipid peroxidation

that was expressed as malondialdehyde (MDA) content by thiobarbituric acid (TBA) assay (Du and Bramlage, 1992). The surface cleaned leaves were used for quantification of percentage electrolyte leakage (% EL) (Lutts et al., 1996). Loss of cell viability was determined by Evans blue staining assay (Baker and Mock, 1994) (details are given as supplementary material as section 2S).

2.5.5. Determination of soluble sugar, soluble protein and thiol content

Soluble sugar in shoots was measured as described by Koehler (1952). The soluble protein was determined according to Bradford (1976) using bovine serum albumin as the protein standard. Thiol content in was determined according to Devi and Prasad (1998).

2.6. Determination of arsenic concentration

The arsenic speciation in all samples was performed according to Le et al. (2000) and concentration of As(III) and As(V) was determined through hybrid generation-atomic fluorescence spectroscopy (HG_AFS; AFS-830, Beijing Jitian Instrument Co., Ltd., Beijing, China). The sample processing and handling before determination is given below. All of the arsenic quantifications were conducted simultaneously, two weeks after experiment.

2.6.1. Arsenic determination in plant tissues and mesocosm

A measured mass of root and shoot samples was oven dried at 80 °C till the constant weight was achieved and, after drying, digested according to aqua regia (3 ml HCl and 1 ml HNO_3) digestion method (Mir et al., 2007). The As(III) and (V) in liquid samples (collected and preserved in section 2.5) were also determined to monitor arsenic fluctuations and %RE in microcosms. (Details are given as supplementary material section 3S)

2.6.2. Arsenic determination in sub-cellular parts of V. denseserrulata

The fresh leaves of the plant were fractioned into cell wall, organelle and soluble fraction by differential centrifugation technique with a few modifications made by Chen et al. (2014). The cell wall and organelle fraction were digested in aqua regia (as mentioned above) and soluble fraction was preserved in 0.5% HNO_3. All samples were stored at −20 °C in dark for arsenic determination (Le et al., 2000).

2.7. FT-IR spectroscopy

The compositional variations in the leaves were studied by FT-IR spectrometer (Nicolet 380, Thermos Scientific Inc., Waltham, MA, USA) at room temperature. Freeze dried leaves along with KBr were made into pallets. Sample scanning was done 64 times from 400 to 4000 cm^{-1} with a resolution of 4 cm^{-1}. The background interference was eliminated and the recorded spectra were analyzed by OMNIC professional software version 8.3.

2.8. Scanning electron microscopy (SEM) analysis of root-bacteria interaction

The roots of the plants were carefully removed, washed with deionized water and fixed in 3% glutaraldehyde for 6 h. After fixation, the samples were washed with serially diluted ethanol (40–100%) and air dried in a sterilized chamber before observation under SEM (Model: JSM-6390LV; NTC, Tokyo, Japan). All of the samples were featured under field-emission SEM with a magnification of 1000 and accelerated voltage of 15 KV.

2.9. Statistical analysis

The analysis of variance (ANOVA) and Duncan multiple range test (DMRT) were executed ($p < 0.05$) using SPSS 19.0 for Window 10 (SPSS Inc., Chicago, IL, USA). All analyses were done in duplicates to calculate mean and standard deviation.

Table 1
Arsenic resistance, reduction and plant growth (PGP attributes of strain XZM).

IAA (μg/ml)	L	162.13 ± 2.12 ($90 \times 10^3 \pm 10$ CFU/ml)
	H	187.21 ± 3.0 ($78 \times 10^3 \pm 16$ CFU/ml)
EPS (μg/ml)	L	0.08 ± 0.01 ($4.6 \times 10^5 \pm 3$ CFU/ml)
	H	0.11 ± 0.01 ($2.8 \times 10^5 \pm 6$ CFU/ml)
Siderosphore	L	Positive
	H	Positive
As reduction	50 mM	67.34% ± 2.16
MIC (mM)	As(III)	≤7.5 ± 0.00
	As(V)	≤85 ± 0.00

H: 2.5 ppm As V, L: 0.25 ppm As V, MIC: minimum inhibitory concentration, IAA: indol-3-acetic acid, EPS: Extracellular polymeric substances, Mean ± Standard deviation.

3. Results

3.1. Arsenic tolerance and PGP attributes of strain XZM

The results of bacterial analyses are shown in Table 1. Bacterium was able to tolerate As(III) and As(V) at concentration levels of ≤7.5 and ≤85 mM respectively, and reduced 67.34% of As(V) to As(III) in 5 mM Na_2HAsO_4 solution. It was able to produce IAA at both arsenic concentrations L and H (162.13 and 287.21 μg/ml respectively) and exhibited a positive siderosphore production. The strain XZM produced 0.08 μg/ml EPS at 0.25 ppm arsenic that was increased to 0.11 μg/ml EPS when arsenic concentration was raised to 2.5 ppm.

3.2. Effect of arsenic stress and bacterial inoculation on growth of V. denseserrulata

V. denseserrulata was planted in microcosms containing Na_2HAsO_4 in 1% Hongland solution for 20 days with 5 treatments named as C, L, LB, H, and HB. The strain *Bacillus* XZM was inoculated in microcosms at an average of 10^8 CFU/ml. After harvesting, the plant growth parameters such as root and shoot length, biomass gain, cell death and chlorophyll content were measured that are presented in Table 2. The growth pattern of plant in all microcosms can be seen more clearly in photograph presented as Fig. 5d. It was observed that *V. denseserrulata* was able to grow well in treatment L without any significant ($p \leq 0.05$) growth inhibition while at the same time in group H, its growth was not only inhibited but a considerable ($p \leq 0.05$) reduction of 26.21% was also recorded in its biomass that was further confirmed by %EB retention. The leaves of harvested plant in this particular microcosms retained significantly higher amount (151%) of Evans blue dye that represented maximum cell death ratio among all microcosms. Meanwhile, inoculation with *Bacillus* XZM significantly ($p \leq 0.05$) increased the biomass by 24.19% and 21.99% in LB and HB, respectively. The chlorophyll contents in LB and HB treatments were also higher than L and H, respectively.

3.3. Biochemical response of V. denseserrulata against arsenic stress

The MDA concentration and %EL in plant roots and shoots is shown in Fig. 1a and b. The LB and HB showed a considerably ($p \leq 0.05$) lower MDA content than L, H, and C. The shoots contained more MDA content than roots. Similar trend was observed in the case of EL with the only difference that C showed lowest %EL. The significant ($p \leq 0.05$) change in soluble protein, soluble sugar and thiol was also recorded as a result of *Bacillus* XZM inoculation (as provided in Fig. 4 b, c and d, respectively). Thiol and soluble sugar content were increased with increasing arsenic accumulation while a reverse effect was monitored for soluble protein content. Moreover, the inoculation of *Bacillus* XZM in LB and HB considerably increased the protein content compared

Table 2
Morphological properties and growth of *Vallisneria denseserrulata* harvested from microcosms after 20 days.

	RL	SL	FB	DB	Chlorophyll		BG	EB	TN	TP
	(cm)	(cm)	(g)	(g)	A	B	(%)	(%)	mg/g	mg/g
C	$13.21^{b} \pm 1.20$	$35.13^{c} \pm 0.34$	$15.31^{b} \pm 0.31$	$1.63^{b} \pm 0.17$	$0.36^{c} \pm 0.01$	$0.49^{c} \pm 0.01$	$21.39^{c} \pm 1.21$	$88.22^{b} \pm 1.31$	$59.22^{c} \pm 2.11$	$9.83^{c} \pm 0.86$
LB	$16.16^{d} \pm 0.21$	$38.52^{e} \pm 1.43$	$22.12^{d} \pm 0.35$	$2.19^{d} \pm 0.13$	$0.65^{d} \pm 0.01$	$0.89^{e} \pm 0.02$	$24.33^{d} \pm 1.43$	$86.36^{a} \pm 1.04$	$61.45^{d} \pm 1.95$	$8.94^{b} \pm 0.92$
L	$14.70^{c} \pm 0.70$	$33.31^{b} \pm 1.31$	$20.45^{c} \pm 0.43$	$2.08^{c} \pm 0.21$	$0.28^{b} \pm 0.03$	$0.33^{b} \pm 0.01$	$16.03^{b} \pm 1.32$	$92.52^{c} \pm 1.21$	$54.15^{b} \pm 3.12$	$7.56^{a} \pm 0.84$
HB	$14.23^{c} \pm 0.31$	$36.43^{d} \pm 0.89$	$21.5^{d} \pm 1.32$	$2.26^{e} \pm 0.16$	$0.63^{d} \pm 0.02$	$0.82^{d} \pm 0.03$	$21.99^{c} \pm 0.21$	$88.31^{b} \pm 1.63$	$58.06^{c} \pm 2.16$	$9.74^{c} \pm 0.48$
H	$5.62^{a} \pm 0.12$	$26.28^{a} \pm 1.21$	$10.99^{a} \pm 0.42$	$1.08^{a} \pm 0.23$	$0.19^{a} \pm 0.02$	$0.29^{a} \pm 0.02$	$-26.21^{a} \pm 1.3$	$151.68^{d} \pm 1.36$	$46.31^{a} \pm 2.45$	$7.61^{a} \pm 0.32$

RL: root length, SL: shoot length, FM: fresh biomass, DB: dry biomass, BG: biomass-gain EB: Evans blue uptake.
Note: Mean ± Standard deviation (n = 2) and alphabets (abc) denote value of significant diff ;erences compared to the corresponding control value according to DMRT. at $p \leq 0.05$.

with L and H, respectively.

3.4. FTIR spectroscopy of plant leaves

The evaluation of FT-IR spectra from 4000 to 400 cm^{-1} of harvested leaves from microcosms C, L, LB, H, and HB (Fig. 4) exhibited a variety of transmission peaks, reflecting the compound nature of *V. denseserrulata*. Similar intensities were observed for C, LB and HB while, intensity pattern of H and L was similar to each other. The significant shift of the peaks at 3335, 2925, 1385, 1137, and 619 cm^{-1} was observed in the transmittance spectra.

3.5. Arsenic accumulation and speciation in plant tissues

The arsenic accumulation in shoots and roots of the *V. denseserrulata* is given in Fig. 2a and b respectively, that clearly depicted the bioaccumulation of arsenic (collectively for shoots and roots; > 1500 mg/Kg in HB) in the plant, while most of it was present in shoots. Inoculating microcosms with XZM significantly ($p \leq 0.05$) enhanced the arsenic accumulation, in plant, in LB and HB compared with L and H, respectively. In plant tissues, most of the arsenic was (> 85%) was in the form of As(III) and it was more or less same for all treatments. Furthermore, the results of subcellular distribution of arsenic in shoots are given in Fig. 3 a and its speciation is presented in Fig. 3b. About 69–77% of the total arsenic was present in soluble fraction, while < 15 of the total arsenic was found in cell wall. In soluble fraction, > 95% of arsenic was present in the form of As(III) and similar trend was observed in cell wall and organelle fraction.

3.6. Strain XZM association with V. denseserrulata roots

The adherence and matrix formation ability of the strain XZM on plant roots are shown in SEM images, presented in Fig. 5a, b and c for LB, HB and C, respectively. The association of the strain *Bacillus* XZM with plant roots in treatment LB and HB, while its absence in the case of C is a clear indicative of the phenomena that bacterium was responsible for enhanced plant growth and arsenic uptake.

3.7. Phytobial remediation of arsenic in microcosms

The arsenic speciation and %RE in microcosms are presented in Figures S_1 and 6 respectively. In treatments LB and HB, a considerable arsenate reduction was measured (S_1a and S_1b) while on the other hand most of the arsenic was in the form of As(V) (S_1c and S_1d) in L and H. The %RE was the lowest in H among all microcosms while the LB and HB showed high arsenic removal of 93 and 97%, correspondingly. Most of the arsenic removal was achieved with in first 12 d of the experiment.

4. Discussions

Vallisneria are well known for arsenic accumulation directly from aquatic medium such as *Vallisneria neotropicalis* (Lafabrie et al., 2011), *Vallisneria natans* (Lour.) Hara (Chen et al., 2017) and *Vallisneria gigantean* (Iriel et al., 2015). At the best of our knowledge, the arsenic accumulation and its detoxification mechanism in *V. denseserrulata* have not been reported before. This plant is native to Middle East and East Asia and its leaves can grow up to the length of one meter. Moreover, its growth is less temperature and light sensitive (Zhi et al.,

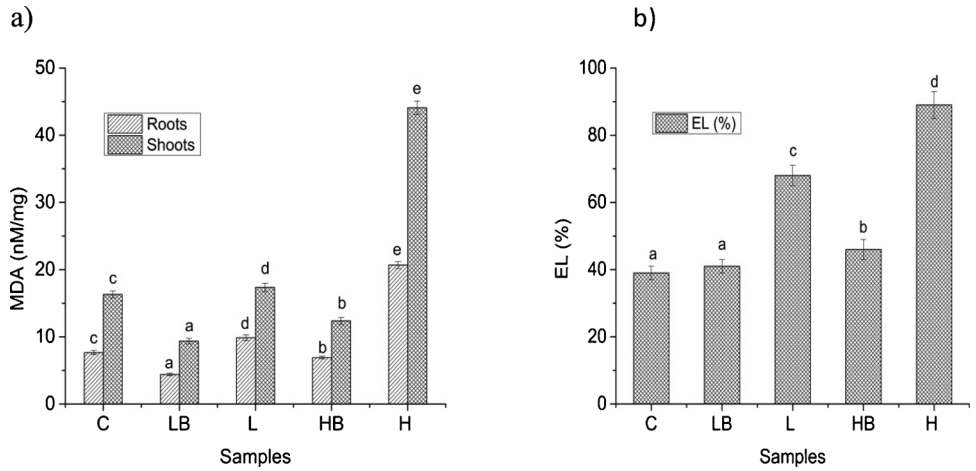

Fig. 1. Oxidative stress on *V. denseserrulata* in different microcosms; 1a: malondialdehyde contents, 1b: Electrolytic leakage.
Note: Error bars indicate standard deviation (n = 2) and alphabets (abc) denote a value of significant diff ;erences compared to the corresponding control value according to DMRT. at $p \leq 0.05$.

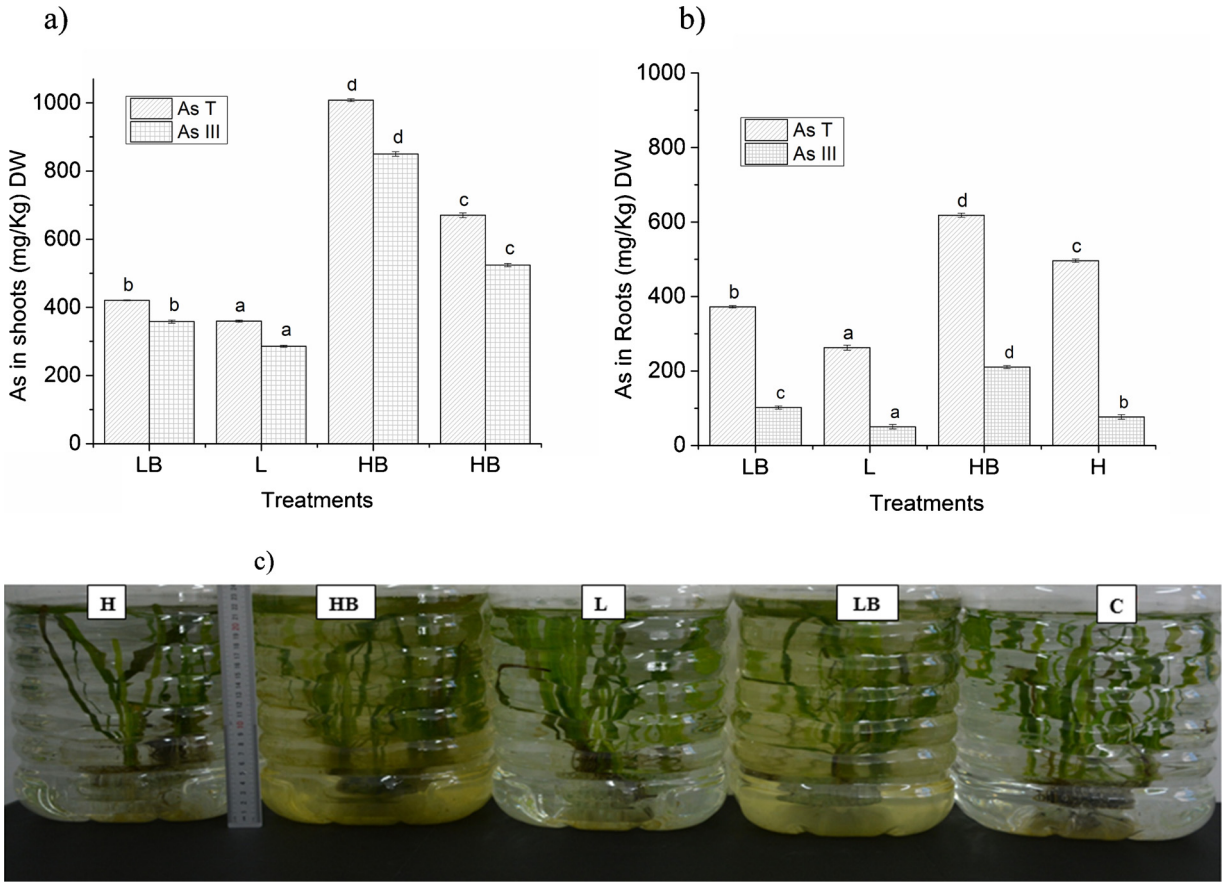

Fig. 2. Arsenic speciaction in roots and shoots of *V. denseserrulata* in different microcosms; 2a) Arsenic in shoots, 2b). Arsenic in roots and2c) Microcosms after experiment.
Note: Error bars indicate standard deviation (n = 2) and alphabets (abc) denote a value of significant diff ;erences compared to the corresponding control value according to DMRT. at $p \leq 0.05$.

2018). These abilities make this specie favorable to be trailed for arsenic phytoremediation in a variety of environmental conditions (Prum et al., 2018).

4.1. Influence of arsenic stress and Bacillus XZM on V. denseserrulata

The results revealed that *V. denseserrulata* accumulated arsenic; although arsenic was toxic and inhibited the plant growth at 2.5 ppm in H microcosm still it was able to tolerate 0.25 ppm of arsenic (Table 2). There have been alike reports of reduced plant growth under arsenic stress such as red clover (Mascher et al., 2002), *Pteris vittata* (Ma et al., 2001), and *Holcus lanatus* L. (Hartley-Whitaker et al., 2001). The photosynthetic apparatus is considered as most sensitive and important bio-indicator of abiotic stress in arsenic hyper-accumulators (Chen et al., 2014).

In the current study, reduced photosynthetic pigments and protein content under arsenic stress (L and H) might be due to MDA production as a result of oxidative stress (Fig. 1a). Similar inferences are reported by Singh et al. (2007) while reporting arsenic induced growth inhibition in *Phaseolus aureus*. The toxicity was also linked with the electrolytic imbalance (Fig. 1b), cell death (Table 2), reduced protein content (Fig. 4b) and increased sugar (Fig. 4c).

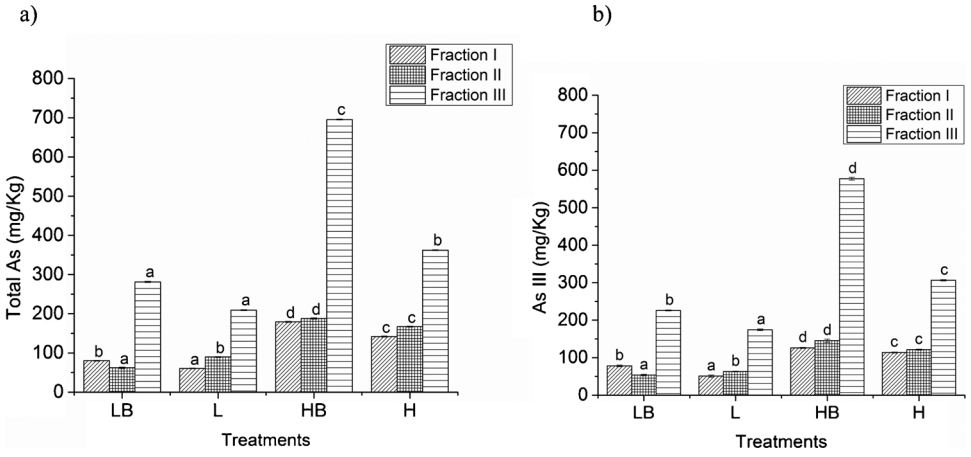

Fig. 3. Arsenic speciation in subcellular parts of *V. denseserrulata;* 3a) Total arsenic (mg/kg) at subcellular level in shoots, 3b) As(III) in subcellular fractions.
Note: Error bars indicate standard deviation (n = 2) and alphabets (abc) denote a value of significant diff ;erences compared to the corresponding control value according to DMRT. at $p \leq 0.05$.

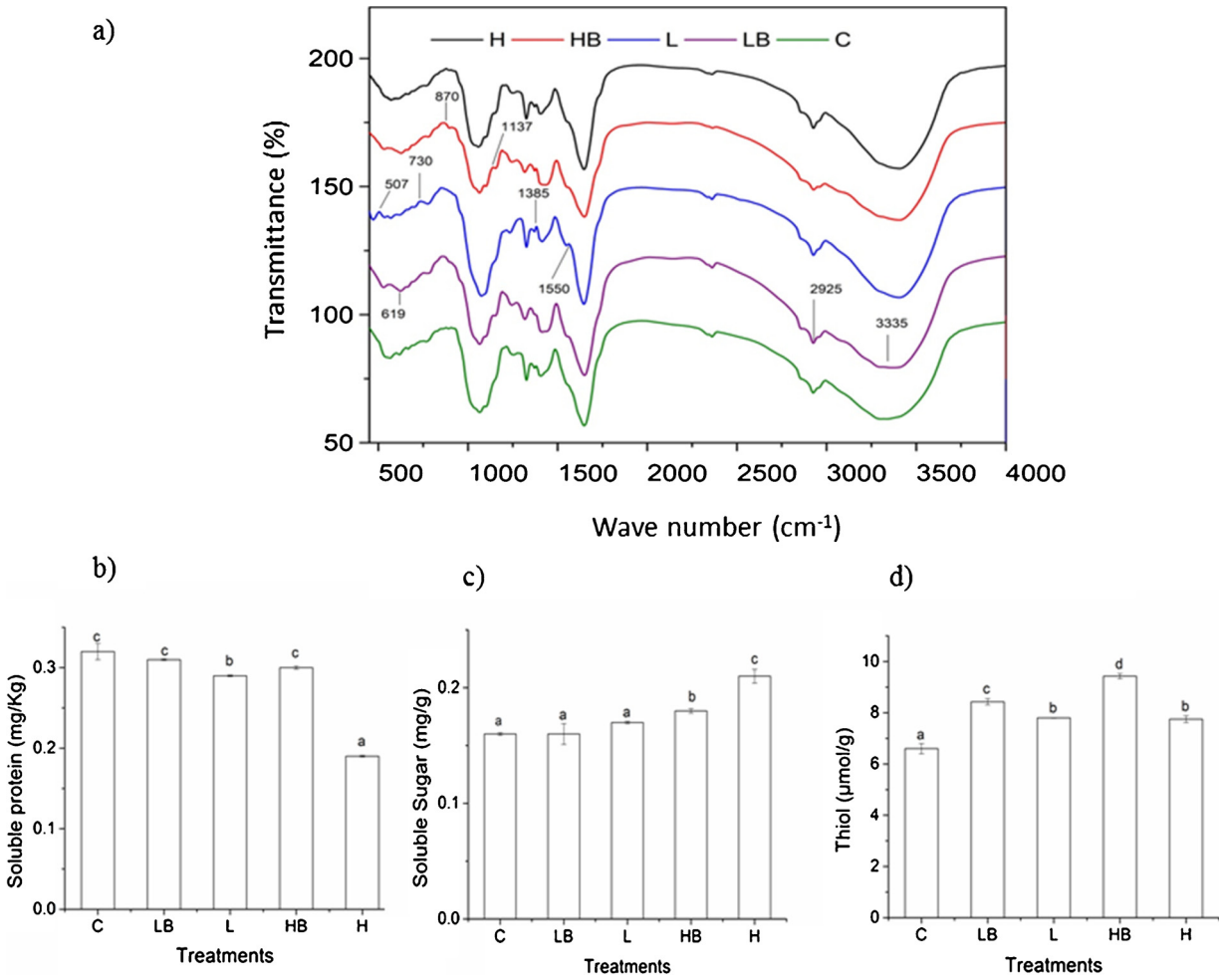

Fig. 4. Chemical changes in *V. denseserrulata* shoots as a result of arsenic stress. 4a) FT-IR transmission spectra 4b) soluble protein content, 4c) fluctuations in Soluble sugar content and 4d) Thiol content in leaves of *V. denseserrulata* shoots.
Note: Error bars indicate standard deviation (n = 2) and alphabets (abc) denote a of value significant diff ;erences compared to the corresponding control value according to DMRT at $p \leq 0.05$.

The cell membrane of the plant is seen as a primary target site of heavy metal toxicity and oxidative stress. It is decomposed under stress conditions that can cause EL and even cell death. MDA might have produced during this decomposition (Nie et al., 2002). Lesser amount of MDA in roots and shoots of plants in treatment LB and HB than L, H and C inferred that inoculation of *Baccilus* sp. XZM in microcosms reduced arsenic stress and enhanced the growth of *V. denseserrulata* (Fig. 3a). The PGP bacteria are also well known to reduce the ROS production (Singh et al., 2007; Kidwai et al., 2019), that might have resulted lesser lipid peroxidation (MDA), EL and soluble sugar content (Mascher et al., 2002) in *V. denseserrulata*. The role of bacteria in reducing ROS accumulation might be attributed to the bacterial PGP attributes (mainly IAA production) (Table 1) that effectively reduced arsenic toxicity to the *V. denseserrulata* by reducing oxidative stress. Briefly, as a result of *Baccilus* sp. XZM inoculation, reduced ROS accumulation might have caused lesser EL of in *V. denseserrulata,* which finally resulted in a decreased MDA and an increased chlorophyll and protein content. Hence, the growth of *V. denseserrulata* was improved as result of *Baccilus* sp. XZM inoculation, which is supported by the previous reports as well (Ma et al., 2001; Yang et al., 2012; Prum et al., 2018).

4.2. FT-IR sepectra of V. denseserrulata leaves

The FT-IR spectroscopy of leaves harvested from microcosms C, L, LB, H, and HB was conducted to explore more about arsenic detoxification mechanisms in *V. denseserrulata.* There were significant variations without deceptive bio-chemical variances in the FT-IR metabolic fingerprints of bacterial inoculated leaves as compare to non-inoculated ones (Fig. 4). A resilient and broad transmissions peak at 3335 cm^{-1} showed the stretching of the −N−H bond of amino groups that is also a suggestive of bonded hydroxyl group (Yang et al., 2009). This peak shuffle is further verified by results of soluble protein as provided in Fig. 4b. Amino acids and carboxylic acids (e.g. histidine, proline, citric acid and malic acid) are considered as a ligand for heavy metal detoxification, in plants, the heavy metal tolerance is observed to increase with increasing amino acid content and vice versa (Szabados and Savoure, 2010). The significant intensity difference at about 2925 cm^{-1} in inoculated and non-inoculated arsenic leaves might be allocated to $-CH_2$ stretching of $-CH_2$ and $-CH_3$ that are functional groups in the lipid complexes, and depicted the shift in the methylation pattern in both groups. It might be an indication of cell membrane damage that is further conformed by MDA content fluctuations in plants (Fig. 1a). Significantly shuffled intensity of the band at around 1137 cm^{-1}, representing stretching of C−O−P and C−O−C, recommended that carbonyl groups may be associated with arsenic detoxification and the amide peak at 1550 cm^{-1}, further reinforcing that carbonyl groups might have assisted arsenic detoxification. The transmittance peak at 1385 cm^{-1} may be from the -C-H vibration of carbohydrates. To further support this band stretching, the variation in soluble sugar content is given in Fig. 4c. The bands at < 880 cm^{-1} are

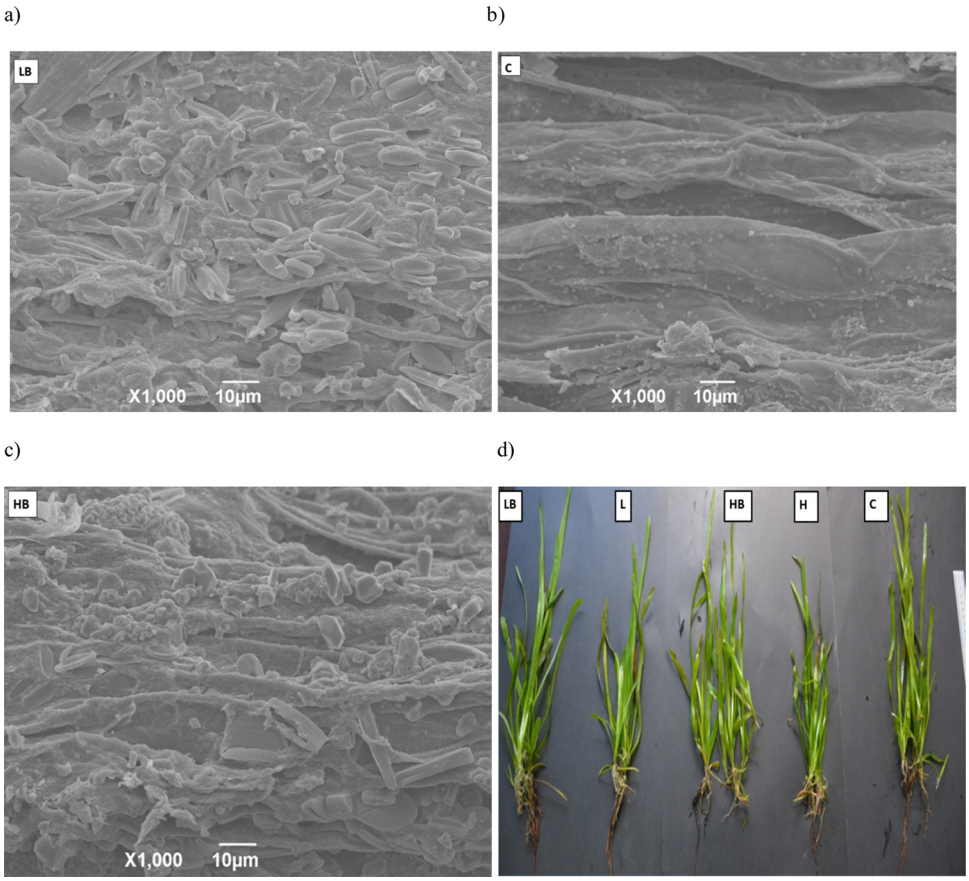

Fig. 5. The growth of *V. denseserrulata* and root association of bacterium XZM; 5a) bacterial growth on roots of plant in microcosm LB, 5b) absence of bacterial growth on roots of control plants, 5c) bacterial growth on roots in HB microcosm, 5d) bacterial enhanced growth of *V. denseserrulata.*

designated as zone for sulfur and phosphate functional groups (da Luz, 2006) which are related with variations of thiol content (Fig. 4d) and TP (Table 1) under different arsenic stress conditions (Chen et al., 2017). The shift of the peaks at 3335, 2925, 1385, 1137, 1550 and 619 cm^{-1} and increase/decrease in the SP, SS, thiol, MDA, TP, and TN as a result of arsenic accumulation in *V. denseserrulata*, is an indicative of involvement of various functional groups (e.g. thiol, amide, carboxyl, and as well as hydroxyl) in metabolisation of arsenic ions, and the existence of an arsenic detoxification process in *V.denseserrulata* leaves.

4.3. Possible mechanism of arsenic detoxification in V. denseserrulata

The symbiotic association between *V. denseserrulata* and *Bacillus* sp. XZM increased the arsenic uptake and accumulation in plant tissues while most of the arsenic was accumulated as As(III) (Fig. 2a and b). The uptake of arsenic in plants is still not very clear, but for most of the aquatic plants direct absorption/bio-sorption is considered as prominent process in this respect (Iriel et al., 2015). The mechanism of arsenic detoxification in plant is complex and multifactorial. The possible mechanism of cellular bio-transformation and bioaccumulation of arsenic in *V. denseserrulata* is given in Fig. 7. It is inferred that reduction of As(V) to As(III) is one of the significant steps in arsenic detoxification at cellular level in *V. denseserrulata* (3a and 3b) that help in arsenic stress tolerance (Chen et al., 2017; Yang et al., 2009; Meharg and Hartley-Whitaker, 2002). This reduction of As(V) to As(III), *in vitro*, is brought about non-enzymatically by glutathione (Delnomdedieu et al., 1994). The biosynthesis of thiol and other PCs is also observed as a key step in arsenic mobilization at cellular level of *V. denseserrulata* (Fig. 4a, b, c and d). The PCs have been reported as precursor of immediate detoxification in many hyper-accumulator and hyper-tolerant plants such as *Ceratophyllum demersum L.* (Devi and Prasad, 1998), *Phaseolus aureus* (Singh et al., 2007), *Echinodorus cordifolius* (Prum et al., 2018) and *P. vittata* (Yang et al., 2012). It is proposed that, in *V. denseserrulata*, the As-PCs/thiol complex is sequestered into the vacuole. In most of the arsenic hyper-accumulators, its major proportion has also been found to be associated with vacuole (Chen et al., 2014). In our experiment, 69 to 77% of the total arsenic was present in the soluble fraction (Fig. 3a and b). The vacuole is a dynamic organelle occupying up to 90% of plant cell volume in specific cells and is a best proposed organelle for compartmentalization of arsenic in plant cells (Zhi et al., 2018). Moreover, the existence of the As(III) in vacuole (˜90%, Fig. 3b) gives the clues of the existence of vacuolar As(III) transporters in *V. denseserrulata*. These arsenic transporters are most probably similar to the As(III) extrusion pumps in *P. vittata* (Indriolo et al., 2010). Genes ACR3 and ACR3;1 have been isolated, from *P. vittata*, and identified to encode a protein that is similar to ACR3. This protein is responsible for arsenite effluxes in vacuolar membrane. Furthermore, this gene sequence is only present in non-flowering plants, and *V. denseserrulata* is a non-flowering plant. So, there is a possibility that certain kind of gene sequence exists in *V. denseserrulata*, responsible for As(III) efflux in vacuolar membrane.

4.4. %RE of arsenic in microcosms

The inoculation of *Baccilus* sp. XZM significantly increased the arsenic RE in LB and HB as compare to L and H, respectively (Fig. 6). Bacteria first adhered to the roots and after sometimes formed a biofilm on it. The turbidity in microcosms LB and LH as shown in Fig. 2c is an indicative of bacterial growth as well. The rode shape *Baccilus* sp. XZM colonizes can be seen clearly on plant roots in Fig. 5 a and b. The bacterial growth in microcosms resulted in an in enhanced bio-removal of arsenic in LB and HB groups. Our results are further supported by the findings of Sun et al. (2018), Nie et al. (2002), Yang et al. (2012) and

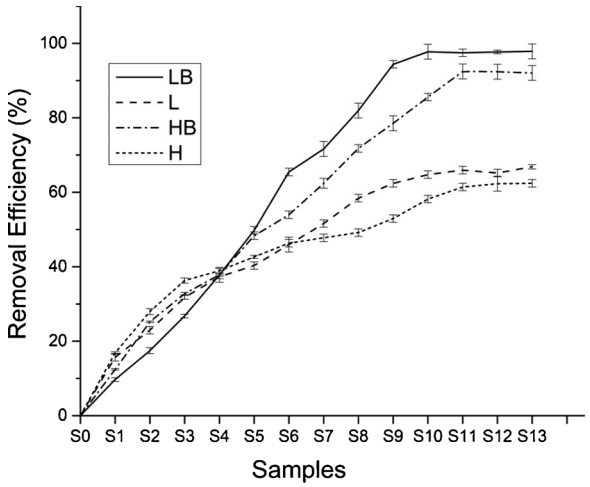

Fig. 6. Arsenic removal efficiency in microcosms.
Note: Error bars indicate standard deviation, and n = 2.

Zhang et al. (2012).

In summary, a successful application of *V. denseserrulata* in arsenic contaminated fresh water ecosystem for bioremediation assisted with indigenous strain *Bacillus* XZM is proved. As this study has focused on the arsenic detoxification in *V. denseserrulata* at subcellular level and exploration of PGP attributes of strain *Bacillus* XZM, the genomics of arsenic metabolism in these organisms still remains a limitation of the current study. There is also a need of further research in the field of finding new plants for arsenic phytoremediation and enhancing the phytoremediation efficiency with the application of indigenous microbes. The use of this microcosmic association in a scale-up constructed wetland is also a future prospect of the study.

5. Conclusion

As a whole, strain *Bacillus* XZM not only produced larger biomass of *V. denseserrulata* but also increased the arsenic phytoavailability, and arsenic removal efficiency was also increased up to 97%. The strain *Bacillus* XZM produced IAA that reduced the ROS accumulation in plant cell as a result lesser MDA production and EL was occurred. Hence, cell death was reduced, while chlorophyll content was increased, and plant grew well even with the high arsenic bioaccumulation.

It was also discovered that vacuole is the sink of arsenic in *V. denseserrulata* shoot cells. Most of the arsenic in *V. denseserrulata* was present in leaves where it was reduced to As(III) and transported to vacuole, possibly, in the form of As-PCs/thiol complexes or as As(III) by vacuolar As(III) transporters. So, complexion (with chemical species containing amide, carboxyl, thiol, and hydroxyl) and vacuolar compartmentalization are major mechanisms of arsenic detoxification in *V. denseserrulata*. It is strongly recommended to use indigenous plants and microbes for arsenic phytobial remediation to eradicate the temporal limitations in the universal application of arsenic phytoremediation.

Acknowledgments

This research was financially supported by the National Natural Science Foundation of China (Grant Nos. 41572230 and 41172219), the Grant for Innovative Research Groups of the National Natural Science Foundation of China (41521001), and the 111 Program (State

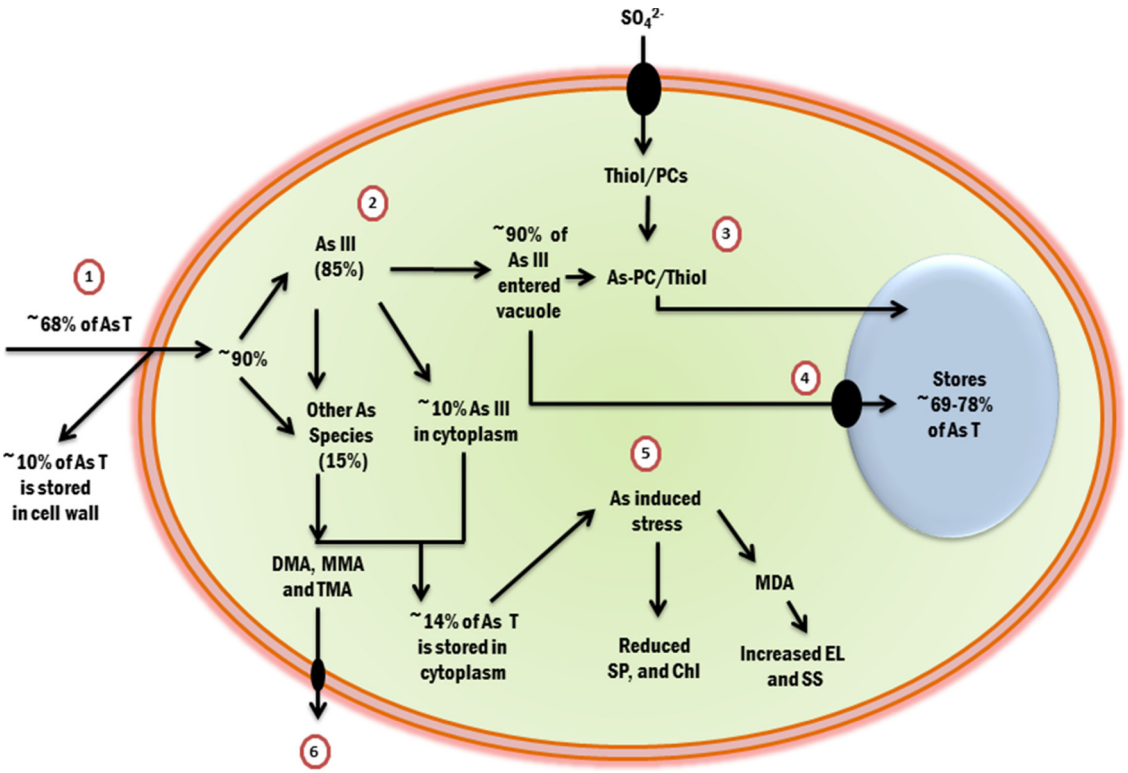

Fig. 7. Possible mechanism of cellular arsenic mobalization in shoots of *V. denseserrulata*.
[1]about 68% of arsenic is trans-located in the shoot/leaf cells of *V. denseserrulata* and approximately 10% of it is bio-accumulated in cell wall and 90% is entered in protoplast, [2]here about 85% is in the form of As(III) through arsenate reductase activity and rest is other species arsenic, [3] the fate of most of (90%) of As(III) is vacuole, and can have two possible ways for this, first it can be detoxified through and association with PCs e.g. Thiol and then transferred to vacuole [4]secondly the tonoplast may have some vacuolar transporters that allow transport of As(III) into the vacuolar sap, [5]rest of As(III) remain in cytoplasm along with other arsenic species e.g. As(V), DMA, MMA and TMA, arsenic also induces stress on the plant cell that is incurred in the form of lipid peroxidation and release of sugar content and [6] finally some of the arsenic may leave plant cell in the form of volatile species of or can re-enter to the root cell.

Administration of Foreign Experts Affairs & the Ministry of Education of China, grant B18049).

Appendix A. Supplementary data

Supplementary material related to this article can be found, in the online version, at doi:https://doi.org/10.1016/j.jhazmat.2019.120903.

References

Soetan, K., Olaiya, C., Oyewole, O., 2010. The importance of mineral elements for humans, domestic animals and plants-A review. Afr. J. Food Sci. Technol. 4, 200–222.

Aljerf, L., 2018. High-efficiency extraction of bromocresol purple dye and heavy metals as chromium from industrial effluent by adsorption onto a modified surface of zeolite: kinetics and equilibrium study. J. Environ. Manage. 225, 120–132.

Duan, G., Zhu, Y., 2018. Arsenic in soil-plant system: a synthesis. Twenty Years of Research and Development on Soil Pollution and Remediation in China. Springer, pp. 453–464.

Rodríguez-Lado, L., Sun, G., Berg, M., Zhang, Q., Xue, H., Zheng, Q., Johnson, C.A., 2013. Groundwater arsenic contamination throughout China. Science 341, 866–868.

W.H. Organization, 2011. Guidelines for Drinking-water Quality. Available on http://apps. who. int/iris/bitstream/10665/44584/1/9789241548151 eng. pdf, (2015).

Mascher, R., Lippmann, B., Holzinger, S., Bergmann, H., 2002. Arsenate toxicity: effects on oxidative stress response molecules and enzymes in red clover plants. Plant Sci. 163, 961–969.

Deng, F., Guo, X., 2011. Association of 5, 10-Methylenetetrahydrofolate reductase polymorphisms, arsenic metabolism, and arsenic skin lesions in residents chronically exposed to arsenic in drinking water. Epidemiol 22, S135.

Chakraborty, S., Bhar, K., Saha, S., Chakrabarti, R., Pal, A., Siddhanta, A., 2014. Novel arsenic nanoparticles are more effective and less toxic than As (III) to inhibit extracellular and intracellular proliferation of *Leishmania donovani*. J. Parasitol. Res. 2014, 187640.

Bertolero, F., Pozzi, G., Sabbioni, E., Saffiotti, U., 1987. Cellular uptake and metabolic reduction of pentavalent to trivalent arsenic as determinants of cytotoxicity and morphological transformation. Carcinogenesis 8, 803–808.

Chen, G., Feng, T., Li, Z., Chen, Z., Chen, Y., Wang, H., Xiang, Y., 2017. Influence of sulfur on the arsenic phytoremediation using Vallisneria natans (Lour.) Hara. Bull. Environ. Contam. Toxicol. 99, 411–414.

Ma, L.Q., Komar, K.M., Tu, C., Zhang, W., Cai, Y., Kennelley, E.D., 2001. A fern that hyperaccumulates arsenic. Nature 409, 579.

Lafabrie, C., Major, K., Major, C., Cebrián, J., 2011. Arsenic and mercury bioaccumulation in the aquatic plant, Vallisneria neotropicalis. Chemosphere 82, 1393–1400.

Hartley-Whitaker, J., Ainsworth, G., Meharg, A.A., 2001. Copper-and arsenate-induced oxidative stress in Holcus lanatus L. Clones with differential sensitivity. Plant Cell Environ. 24, 713–722.

Xie, Z., Sun, X., Wang, Y., Luo, Y., Xie, X., Su, C., 2014. Response of growth and superoxide dismutase to enhanced arsenic in two *Bacillus* species. Ecotoxicol. 23, 1922–1929.

Sun, W., Xiong, Z., Chu, L., Li, W., Soares, M.A., White Jr, J.F., Li, H., 2018. Bacterial communities of three plant species from Pb-Zn contaminated sites and plant-growth promotional benefits of endophytic *Microbacterium sp.*(Strain BXGe71). J. Hazard. Mater. 370, 225–231.

Nie, L., Shah, S., Rashid, A., Burd, G.I., Dixon, D.G., Glick, B.R., 2002. Phytoremediation of arsenate contaminated soil by transgenic canola and the plant growth-promoting bacterium *Enterobacter cloacae* CAL2. Plant Physiol. Biochem. 40, 355–361.

Yang, Q., Tu, S., Wang, G., Liao, X., Yan, X., 2012. Effectiveness of applying arsenate reducing bacteria to enhance arsenic removal from polluted soils by Pteris vittata L. Int. J. phytoremediat. 14, 89–99.

Aljerf, L., AlMasri, N., 2018. A gateway to metal resistance: bacterial response to heavy metal toxicity in the biological environment. Ann. Adv. Chem. 2, 032–044.

Prum, C., Dolphen, R., Thiravetyan, P., 2018. Enhancing arsenic removal from arsenic-contaminated water by *Echinodorus cordifolius* – endophytic *Arthrobacter creatinolyticus* interactions. J. Environ. Manage. 213, 11–19.

Meharg, A.A., Hartley-Whitaker, J., 2002. Arsenic uptake and metabolism in arsenic resistant and nonresistant plant species. New Phytol. 154, 29–43.

Iriel, A., Lagorio, M.G., Cirelli, A.F., 2015. Biosorption of arsenic from groundwater using *Vallisneria gigantea* plants. Kinetics, equilibrium and photophysical considerations. Chemosphere 138, 383–389.

Gordon, S.A., Weber, R.P., 1951. Colorimetric estimation of indoleacetic acid. Plant Phyisol. 26, 192.

Kazy, S.K., Sar, P., Singh, S., Sen, A.K., D'souza, S., 2002. Extracellular polysaccharides of a copper-sensitive and a copper-resistant *Pseudomonas aeruginosa* strain: synthesis, chemical nature and copper binding. World J. Microbio. Biotech. 18, 583–588.

Schwyn, B., Neilands, J., 1987. Universal chemical assay for the detection and determination of siderophores. Anal. Biochem. 160, 47–56.

Le, X.C., Yalcin, S., Ma, M., 2000. Speciation of submicrogram per liter levels of arsenic in water: on-site species separation integrated with sample collection. Environ. Sci. Tech. 34, 2342–2347.

Hoagland, D.R., Arnon, D.I., 1950. The water-culture method for growing plants without soil. Circular. California Agr. Exp. Stat. 347, 1–32.

Horneck, D.A., Miller, R.O., 1997. Determination of total nitrogen in plant tissue. Handbook of Reference Methods for Plant Analysis. CRC Press, pp. 85–93.

Fiske, C.H., Subbarow, Y., 1925. The colorimetric determination of phosphorus. J. Biol. Chem. 66, 375–400.

Maclachlan, S., Zalik, S., 1963. Plastid structure, chlorophyll concentration, and free amino acid composition of a chlorophyll mutant of barley. Can. J. Bot. 41, 1053–1062.

Du, Z., Bramlage, W.J., 1992. Modified thiobarbituric acid assay for measuring lipid oxidation in sugar-rich plant tissue extracts. J. Agr. Food Chem. 40, 1566–1570.

Lutts, S., Kinet, J., Bouharmont, J., 1996. NaCl-induced senescence in leaves of rice (*Oryza sativa L.*) cultivars differing in salinity resistance. Ann. Bot. 78, 389–398.

Baker, C.J., Mock, N.M., 1994. An improved method for monitoring cell death in cell suspension and leaf disc assays using Evans blue, Plant Cell. J. Tissue Cult. Methods 39, 7–12.

Koehler, L.H., 1952. Differentiation of carbohydrates by anthrone reaction rate and color intensity. Anal. Chem. 24, 1576–1579.

Bradford, M.M., 1976. A rapid and sensitive method for the quantitation of microgram quantities of protein utilizing the principle of protein-dye binding. Anal. Biochem. 72, 248–254.

Devi, S.R., Prasad, M., 1998. Copper toxicity in *Ceratophyllum demersum L.*(Coontail), a free floating macrophyte: response of antioxidant enzymes and antioxidants. Plant Sci. 138, 157–165.

Mir, K.A., Rutter, A., Koch, I., Smith, P., Reimer, K.J., Poland, J.S., 2007. Extraction and speciation of arsenic in plants grown on arsenic contaminated soils. Talanta 72, 1507–1518.

Chen, G., Liu, X., Xu, J., Brookes, P.C., Wu, J., 2014. Arsenic species uptake and subcellular distribution in *Vallisneria natans (Lour.) Hara* as influenced by aquatic pH. Bull. Environ. Contam. Toxicol. 92, 478–482.

Zhi, Y., Cao, Y., Sun, J., Li, W., Jeppesen, E., 2018. Indirect effects of extreme precipitation on the growth of Vallisneria denseserrulata Makino. Environ. Exp. Botany 153, 229–235.

Singh, H.P., Batish, D.R., Kohli, R.K., Arora, K., 2007. Arsenic-induced root growth inhibition in mung bean (*Phaseolus aureus Roxb.*) is due to oxidative stress resulting from enhanced lipid peroxidation. Plant Growth Regulat. 53, 65–73.

Kidwai, M., Dhar, Y.V., Gautam, N., Tiwari, M., Ahmad, I.Z., Asif, M.H., Chakrabarty, D., 2019. *Oryza sativa* class III peroxidase (OsPRX38) overexpression in *Arabidopsis thaliana* reduces arsenic accumulation due to apoplastic lignification. J. Hazard. Mater. 362, 383–393.

Yang, X., Chen, H., Dai, X., Xu, W., He, Z., Ma, M., 2009. Evidence of vacuolar compartmentalization of arsenic in the hyperaccumulator *Pteris vittata*. Chin. Sci. Bull. 54, 4229–4233.

da Luz, B.R., 2006. Attenuated total reflectance spectroscopy of plant leaves: a tool for ecological and botanical studies. New Phytol. 172, 305–318.

Szabados, L., Savoure, A., 2010. Proline: a multifunctional amino acid. Trends Plant Sci. 15, 89–97.

Delnomdedieu, M., Basti, M.M., Otvos, J.D., Thomas, D.J., 1994. Reduction and binding of arsenate and dimethylarsinate by glutathione: a magnetic resonance study. Chemico-bio. inter. 90, 139–155.

Indriolo, E., Na, G., Ellis, D., Salt, D.E., Banks, J.A., 2010. A vacuolar arsenite transporter necessary for arsenic tolerance in the arsenic hyperaccumulating fern *Pteris vittata* is missing in flowering plants. Plant Cell 22, 2045–2057.

Zhang, X., Lin, L., Chen, M., Zhu, Z., Yang, W., Chen, B., Yang, X., An, Q., 2012. A nonpathogenic *Fusarium oxysporum* strain enhances phytoextraction of heavy metals by the hyperaccumulator Sedum alfredii Hance. J. Hazard. Mater. 229, 361–370.